Aerosol Science and Technology
Publication details, including instructions for authors and subscription information:
http://www.tandfonline.com/loi/uast20

Deposition of Man-Made Fibers in a Human Nasal Airway

Wei-Chung Su [a] , Jun Wu [a] , Jan C. M. Marijnissen [b] & Yung Sung Cheng [a]
[a] Lovelace Respiratory Research Institute , Albuquerque, New Mexico, USA
[b] Department of Chemical Technology , Delft University of Technology , Julianalaan, Delft, The Netherlands
Published online: 03 Apr 2008.

To cite this article: Wei-Chung Su , Jun Wu , Jan C. M. Marijnissen & Yung Sung Cheng (2008) Deposition of Man-Made Fibers in a Human Nasal Airway, Aerosol Science and Technology, 42:3, 173-181, DOI: 10.1080/02786820801922938

To link to this article: http://dx.doi.org/10.1080/02786820801922938

Aerosol Science and Technology, 42:173–181, 2008

ISSN: 0278-6826 print / 1521-7388 online
DOI: 10.1080/02786820801922938

Deposition of Man-Made Fibers in a Human Nasal Airway

Wei-Chung Su,[1] Jun Wu,[1] Jan C. M. Marijnissen,[2] and Yung Sung Cheng[1]
[1]*Lovelace Respiratory Research Institute, Albuquerque, New Mexico, USA*
[2]*Department of Chemical Technology, Delft University of Technology, Julianalaan, Delft, The Netherlands*

Many occupational lung diseases are associated with exposure to aerosolized fibers in the workplace. The nasal airway is a critical route for fiber aerosol to enter the human respiratory tract. The fiber deposition efficiency in the nasal airway could be used as an index to indicate the fraction of the inhaled fibers potentially transported to the lower airways. In this research, experiments of fiber deposition in the human nasal airway were conducted. Man-made carbon, glass, and titanium dioxide fibers in the inertia regime were used as the test fiber materials. The deposition studies were carried out by delivering aerosolized fibers into a human nasal airway replica at constant human inspiratory flow rates ranging from 15 l/min to 43.5 l/min. The deposition results were compared in detail between these fiber materials to study how the fiber characteristics affected the nasal airway deposition. The results showed that the deposition efficiency of the carbon fiber increases as the fiber impaction parameter increases. Many carbon fibers deposited in the anterior region of the nasal airway. In contrast, very few glass or titanium dioxide fibers deposited in the nasal airway, but relatively more of these two fibers deposited in the turbinate region. This result implies that, if a fiber in the inertia regime is inhaled during normal human breathing, the smaller the fiber, the more easily it could enter the human lower respiratory tract, possibly causing harm to the human respiratory tract.

INTRODUCTION

The study of fiber deposition in the human respiratory tract is essential because adverse health effects might be induced when the fiber is deposited in the lower respiratory tract (Walton 1982; IARC 2002). The nasal airway is the major point of entry for the human respiratory tract, and the deposition fraction found in the nasal airway could directly indicate the remaining fraction of the inhaled fiber that enters the lower respiratory tract. Therefore, understanding the nature of fiber deposition in the nasal airway would substantially assist in studying the hazards caused by the inhaled fibers, and it could also provide useful information for assessing the exposure dosimetry for workers in the fiber industry.

This research carries on our previous study (Su and Cheng 2005) for investigating fiber deposition in the human airway. In that research, man-made carbon fibers with aerodynamic diameters ranging from 8–12 μm (length: 10–300 μm) were used to study the fiber deposition efficiency and deposition pattern in the human nasal airway. A great number of invaluable data as well as much new information regarding the nature of fiber deposition in the nasal airway were acquired from that research. The deposition mechanism for the carbon fibers was defined unambiguously to be impaction, and the fiber's deposition in the nasal airway increases proportionally with the fiber's inertia.

It is known that the fiber aerosol commonly seen in the workplace may vary by the type of fiber manufactory or laboratory (Willeke and Baron 1993; Hesterberg and Hart 2001). Man-made fibers with diverse dimensions and characteristics all have the chance to become aerosolized and suspended in the air, causing risk for the workers in that working environment (Enterline et al. 1987; Baan and Grosse 2004). Therefore, studying fiber deposition in the human airway by using fiber materials with a broad range of dimensions is necessary because the dominant deposition mechanism for different fiber materials might deviate. Although nasal airway particle deposition studies have been conducted intensively with different particle sizes, it has been indicated by Beeckmans (1972) that the deposition data acquired from spherical particles cannot be applied directly to the situation with fiber. To date, very few studies have been published on fiber aerosol deposition in the human nasal airway. There is a notable lack of experimental evidence showing the nature of fiber deposition in the nasal airway for different fiber dimensions. As a consequence, the deposition efficiency and deposition pattern for fibers with different characteristics have remained not well known, not to mention the definability of the deposition mechanisms. In this research, man-made fibers with relatively small diameter and length distributions were used as the test materials. The aerodynamic diameter of the test fibers ranged from 1.8–2.7 μm (length: 2.5–20 μm). Literature has shown that spherical particles with an aerodynamic diameter of approximately 1 μm have low deposition efficiency in the human upper airway

Received 13 July 2007; accepted 16 January 2008.
The authors are grateful to W. T. Fan for technical assistance, and V. Fisher for reviewing this manuscript. This project is sponsored by NIOSH grant RO1 OH003900.
Address correspondence to Wei-Chung Su, Lovelace Respiratory Research Institute, 2425 Ridgecrest Dr. SE, Albuquerque, NM 87108, USA. E-mail: wsu@LRRI.org

(Lippmann 1970, 1977; Heyder and Rudolph 1977; NCRP 1997; Cheng et al. 2001b). Hence, most of the small particles inhaled (including fibers) should be able to pass through the entire nasal or oral airways and then enter the lower respiratory tract. The deposition efficiency and deposition patterns of small fibers in the nasal airway are therefore believed to be different from those of large fibers, such as carbon fibers, as was shown in our previous study (Su and Cheng 2005). In addition, due to the small settling velocity, small fibers have a longer suspension time in the air as small particulates. Thus, the small fibers would have more of a chance, compared with large fibers, to be inhaled and deposited on certain regions of the human lower respiratory tract causing possible lung problems. For these reasons, this research is substantially important for filling the gap mentioned above by presenting the deposition data for small fibers in the human nasal airway. The experimental data acquired from this research has been carefully studied and compared in detail with those obtained from our previous study. In this way, it may greatly help in understanding the differences in the deposition mechanism, deposition efficiency, and deposition pattern attributed to different fiber characteristics. Moreover, all the data obtained can be used to validate available theoretical models to improve the prediction accuracy for the fiber deposition in the nasal airway.

EXPERIMENTAL METHOD

Nasal Airway Replica and Fiber Materials

The human nasal replica used in this research is the same as described in our previous study (Su and Cheng 2005). The entire nasal replica contains 77 1.5-mm acrylic plates and consists of the nasal airway structures from the anterior region (first 25 plates), turbinate region (middle 32 plates), to the posterior region (last 20 plates). Silicon oil was applied to the inside surface of the replica prior to the deposition experiment to ensure the fibers remained in the region where they were deposited.

In our previous study, man-made carbon fiber was used as the test fiber material for the deposition experiment. Parameters for the carbon fiber are described in detail in Su and Cheng (2005). In this research, two new man-made fiber materials were used in conducting the deposition experiments: titanium dioxide (TiO_2) and glass. The TiO_2 fiber used in this research was made at the University of Florida by electro-spinning technology. The TiO_2 fiber is monodisperse in diameter (CMD $= 0.59$ μm, $\sigma_g = 1.18$) and polydisperse in length (CML $= 3.20$ μm) with a density of 4.23 g/cm^3. The glass fiber (JM475/100, Johns Manville Co., Littleton, CO) is nearly monodisperse in diameter (CMD $= 0.62$, $\sigma_g = 1.30$) and polydisperse in length (CML $= 7.67$ μm) with a density of 2.56 g/cm^3. Figure 1 shows images of these three man-made fibers under an optical microscope, and a comparison between the physical characteristics of these three man-made fibers is shown in Table 1 (all the measured data were obtained after the fiber materials passed through the aerosol generation devices). The calculation of the fiber aerodynamic diameter (d_{ae}) is also shown in our previous study based on the equations from Stöber (1972). The estimated d_{ae} for TiO_2 fiber is approximately 2.1–2.7 μm, and the d_{ae} is 1.8–2.3 μm for the glass fiber. The comparison of the estimated d_{ae} for these three fiber materials, including the carbon fiber, is also shown in Table 1.

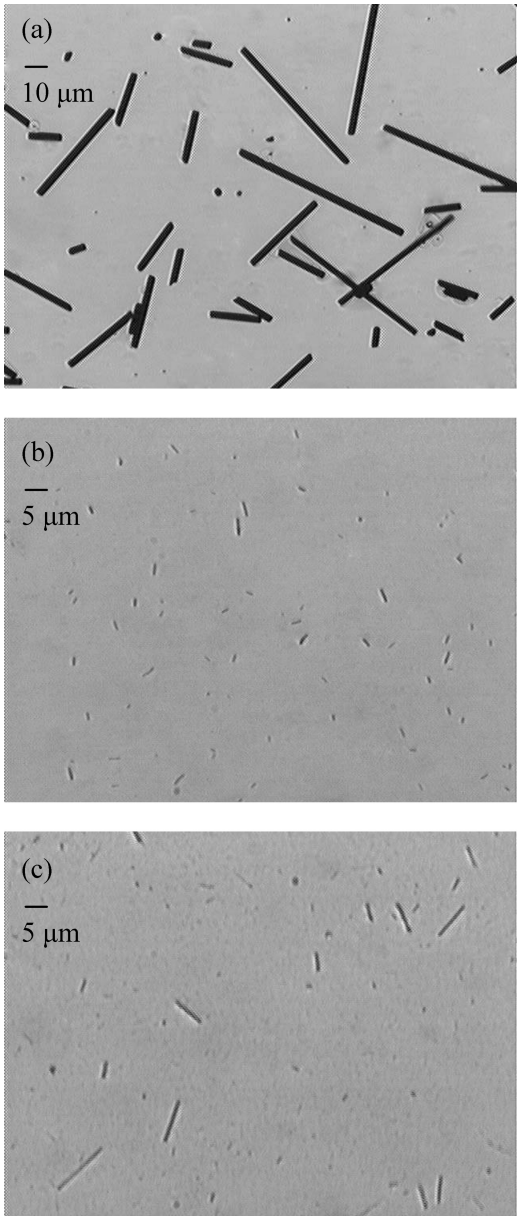

FIG. 1. The test man-made fiber materials (a) carbon fiber, (b) TiO_2 fiber, and (c) glass fiber.

Experimental Setup and Fiber Measurement

Two different methods were used in this research to generate the fiber aerosol. The glass fiber was aerosolized by a small-scale powder disperser (SSPD, Model 3433, TSI Inc., St. Paul, MN), which is the same way the carbon fiber was aerosolized in our previous study. The experimental setup regarding the glass fiber deposition study is identical to that described in Su

TABLE 1
Comparison of the physical characteristics for different man-made fiber materials

Fiber Type	Density	Diameter	Length	d_{ae}^{a}
Carbon	1.83 g/cm^3	CMD = 3.66 μm $\sigma_g = 1.11^b$	CML = 14.83 μm $\sigma_g = 4.00$	7.6–12.8 μm (L = 10–300 μm)
TiO_2	4.23 g/cm^3	CMD = 0.59 μm $\sigma_g = 1.18$	CML = 3.20 μm $\sigma_g = 1.52$	2.1–2.7 μm (L = 2.5–12.0 μm)
Glass	2.56 g/cm^3	CMD = 0.62 μm $\sigma_g = 1.30$	CML = 7.67 μm $\sigma_g = 1.57$	1.8–2.3 μm (L = 3.5–20.0 μm)

[a] Aerodynamic diameter.
[b] Geometric standard deviation.

and Cheng (2005). The TiO_2 fiber aerosol was generated by a medication nebulizer (Up-Mist, Hospitak Inc., Farmingdale, NY). The TiO_2 fiber material plates were placed in alcohol and ultrasonicated for 30 s before the aerosol generation process. Figure 2 shows the experimental setup for the TiO_2 fiber deposition study. The TiO_2 fiber aerosol along with the alcohol droplets generated by the nebulizer was first transferred to several drying columns and a Kr^{85} charge neutralizer prior to entering the nasal airway replica. In this way, sufficient time was provided to ensure that the alcohol mist evaporated and only TiO_2 fiber aerosol remained. The deposition studies for the TiO_2 and the glass fibers were conducted at constant human inspiratory flow rates (Q) ranging from the resting state (15 l/min) to that of light exercise (43.5 l/min). Two experiments were conducted for each inspiratory flow rate to acquire average deposition values. The post-experiment process for preparing the sample slides of the deposited fibers was also the same as described in our previous study (Su and Cheng 2005). The fiber diameter and fiber length distribution were measured manually using an optical microscope. In this research, only TiO_2 fibers longer than 2.5 μm and glass fibers longer than 3.5 μm were counted as the deposition data due to the limitation of the visual measurement.

RESULTS

Figure 3 shows the deposition efficiency as a function of the impaction parameter (fiber momentum) for different man-made fiber materials in the nasal airway replica. The fiber deposition efficiency is defined as the ratio of the fiber number deposited in

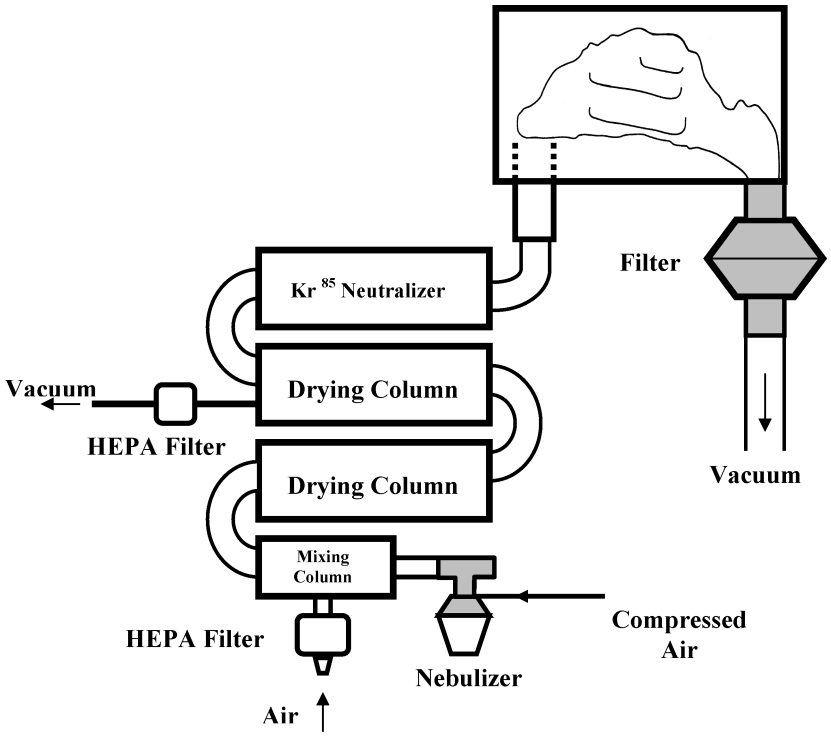

FIG. 2. Schematic diagram of the experimental setup for the TiO_2 fiber deposition study.

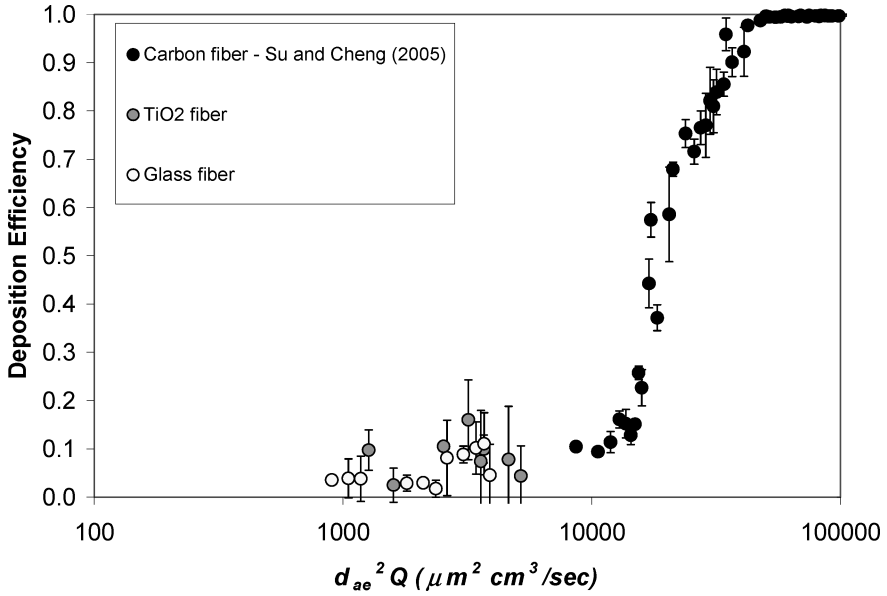

FIG. 3. Deposition efficiency as a function of the impaction parameter for different man-made fiber materials in the human nasal airway.

the nasal airway to the fiber number that entered the nasal airway (i.e., fibers deposited in the nasal airway replica together with fibers collected on the backup filter). The d_{ae} used for calculating the impaction parameter $d_{ae}^2 Q$ is the fiber aerodynamic diameter in random orientation. As can be seen in Figure 3, the trend of the fiber deposition efficiency in the nasal airway is a smooth S-like shape. The lower end of the carbon fiber deposition efficiency is ideally connected to the higher end of the TiO_2 fiber deposition efficiency, which plainly shows the overall continuity between the data sets acquired. Also shown in Figure 3, the deposition efficiency of the carbon fiber increased proportionally with the impaction parameter. This result indicates that impaction is the main deposition mechanism for the carbon fiber used. The deposition efficiency of the carbon fiber can reach 1.0 when the impaction parameter is greater than 50,000 $\mu m^2 cm^3/s$. To the contrary, there was no significant relationship found between the impaction parameter and the deposition efficiency for the TiO_2 and the glass fibers. The deposition efficiencies increased only slightly with an increase in the impaction parameter. In general, the impaction parameters of TiO_2 and glass fibers were both smaller than 6,000 $\mu m^2 cm^3/s$, and partially overlapped. Their deposition efficiencies were shown to be similar, and were both less than 0.2.

Figure 4a and b shows the deposition patterns of different man-made fibers in the human nasal airway for various length categories and inspiratory flow rates. The nasal airway was divided into three major subregions—anterior, turbinate, and posterior, for presenting the deposition pattern in a simple manner. As can be seen, the anterior region is the site of preferred deposition for both short and long carbon fibers. In general, the deposition fraction in the anterior region increases as the inspiratory flow rate increases, and the longer the carbon fiber, the higher the deposition fraction in that region. Besides the anterior region, a considerable number of carbon fibers deposited in the turbinate region, but very few carbon fibers deposited in the posterior region. In contrast, for the TiO_2 and glass fibers, although the total deposition number in the nasal airway is small, relatively more fibers deposited in the turbinate region instead of the anterior region. The regional deposition fractions of the TiO_2 and glass fibers do not substantially change with different fiber length categories, or with an increase in the inspiratory flow rate.

DISCUSSION

Effect of Fiber Characteristics

As shown in Table 1, the carbon fibers have a considerably larger diameter and length distribution compared with the TiO_2 and the glass fibers. This significant difference in the physical dimension gives the carbon fiber a larger d_{ae} value and high inertia. As a result, the impaction parameter as well as the associated deposition efficiency increases substantially when the fiber d_{ae} is increased. The deposition efficiency trend for carbon fiber (Figure 3) shows that most of the high momentum fibers have a deposition efficiency of 1.0, which implies that high momentum fibers do not pass easily through the nasal airway. Thus, the human nose appears to function well for filtering out large particles such as the carbon fibers by preventing them from entering the lower respiratory tract. On the other hand, the dimensions of the TiO_2 and the glass fibers are relatively small compared with the carbon fiber. Therefore, the fiber d_{ae}, the associated impaction parameter, and the fiber deposition efficiency are all consequently small. As shown in Figure 3, The deposition efficiencies of the TiO_2 and the glass fibers all ranged from 0.02–0.2, which implies that small fibers have a high penetration rate

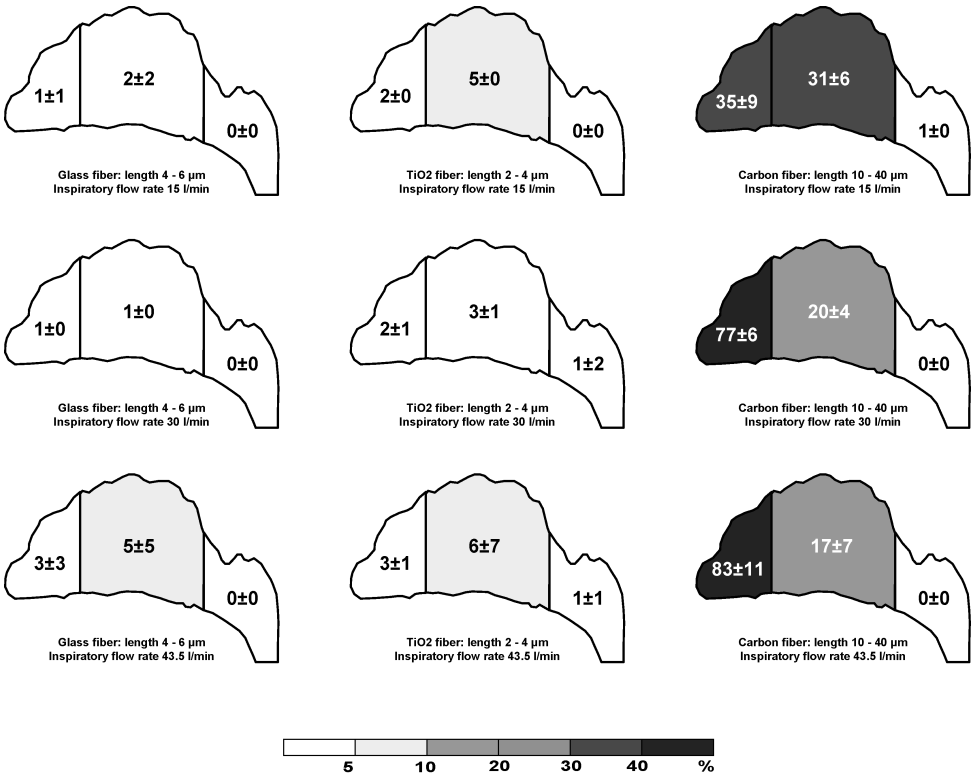

(a)

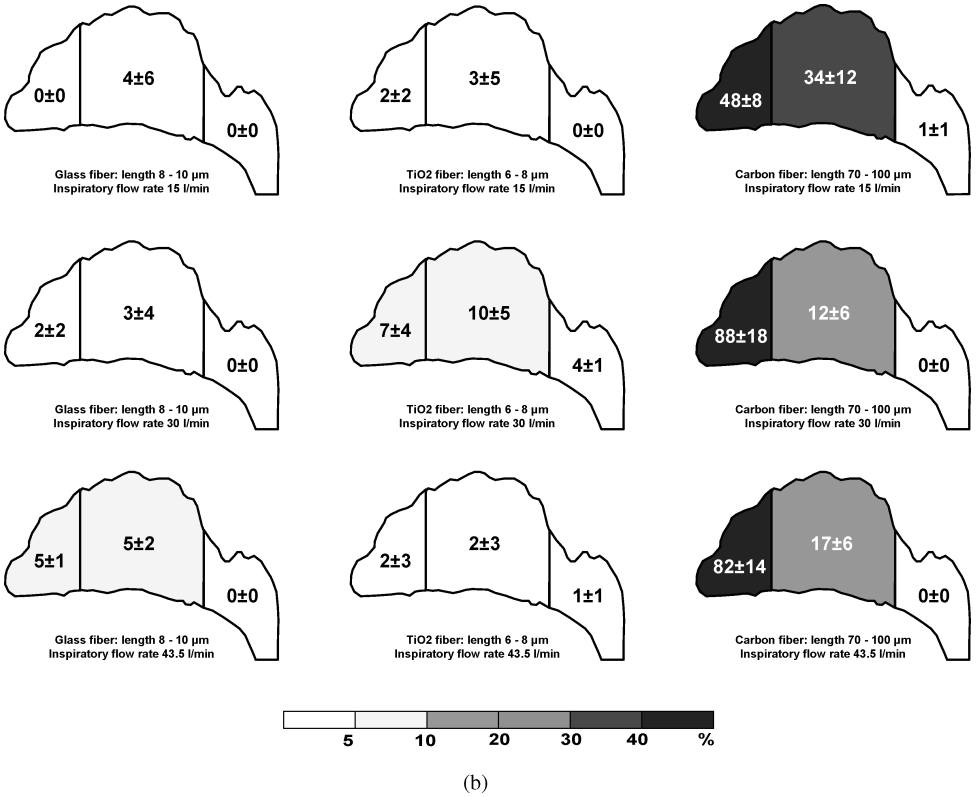

(b)

FIG. 4. Comparison of fiber deposition patterns in the human nasal airway (a) the relatively short fibers in each fiber material, and (b) the relatively long fibers in each fiber material.

($\geq$0.8) through the nasal airway. Therefore, they may present a hazard to the human lower respiratory tract. It is worth noting that the diameters of the TiO_2 and the glass fibers are comparable, and the length distribution of the TiO_2 fiber is shorter than that of the glass fiber. However, the calculated d_{ae} and the related impaction parameters of the TiO_2 fiber are, in general, larger than those of the glass fibers. This result is due to the facts that the density of the TiO_2 fiber is greater than that of the glass fiber and, moreover, the d_{ae} of a fiber depends primarily on its diameter and only slightly on its length (Stöber et al. 1970; Timbrell, 1982; Cheng 1995). As a result, the TiO_2 fiber shows a relatively higher momentum in the nasal airway compared with the glass fiber, and the deposition efficiencies of the TiO_2 fiber agree well with those of the glass fiber where the values of the impaction parameters for these two fibers overlap.

Regional Deposition

The deposition patterns shown in Figure 4 indicate that carbon fibers tend to deposit in the anterior region, but this deposition phenomenon does not hold for the TiO_2 and the glass fibers. This result suggests that the anterior region is the first line of defense for the nasal airway. The anterior region works as an impactor to block out those high momentum fibers or particles inhaled to prevent them from entering the main nasal passage. As stated in our previous study, the 90-degree turn in the anterior region (from vertical to horizontal) is the key factor that leads to the deposition of most high momentum fibers, such as carbon fibers, in this area. This is because most of the fibers with high momentum have difficulty in making the turn with the air flow in the anterior region. Conversely, small fibers have low inertia; therefore, they can follow the air stream closely and then easily make the turn and pass through the anterior region. Therefore, much less deposition was found in this anterior region for TiO_2 and glass fibers as shown in Figure 4.

It has been shown that the turbinate region has a large surface area and complicated airway (Proctor 1982; Mygind 1985). There are three meatuses in the turbinate region: superior turbinate, middle turbinate, and inferior turbinate. In the medium to high inspiratory flow rate the airflow profile in the turbinate region might be turbulence (Swift and Proctor 1977; Cole 1982; Zamankhan et al. 2006), which could cause the turbulent deposition of inhaled particles in this turbinate region. In order to study fiber deposition in the turbinate region, it is necessary to show the deposition fraction in the turbinate region together with its regional deposition efficiency. Here, the regional deposition efficiency is defined as the ratio of the fibers deposited in the specific region of the nasal airway to those that entered that specific region. Table 2 summarizes the calculated regional deposition efficiencies for carbon, TiO_2, and glass fibers in the nasal airway based on the deposition fractions shown in Figure 4. As can be seen, for carbon fibers, the turbinate deposition fractions were generally smaller than the anterior deposition fractions. To the contrary, the turbinate deposition efficiencies of the carbon fiber were shown to be significantly higher than the anterior deposition efficiency. For instance, the anterior deposition fraction of the long carbon fibers (70–100 μm) with a 30 l/min inspiratory flow rate was 87.7% as shown in Table 2, which is much larger than the turbinate deposition fraction of 11.8%. In contrast, the corresponding anterior deposition efficiency was 0.88, which is less than the turbinate deposition efficiency 0.96 under the same condition. However, this difference between the regional deposition fraction and regional deposition efficiency was not shown to be noticeable for the TiO_2 and the glass fibers. The possible reason might be that there were only a few TiO_2 and glass fibers deposited in the nasal airway. Therefore, the comparison between the regional deposition fraction and regional deposition efficiency in the anterior and turbinate regions was not significant. Nevertheless, both the deposition fraction and deposition efficiency in the turbinate region were shown to be larger than those in the anterior region. Therefore, it can be concluded that the turbinate deposition efficiencies were generally larger than the anterior deposition efficiencies for all fiber materials in the nasal airway. This also confirms that the turbinate region is capable of high efficiency deposition for fibers or other inhaled particles by turbulent deposition, especially for those with high momentum. This capability is very advantageous for nasal airway drug delivery, such as using nasal spray to deliver drug-containing particles in the turbinate region. However, some pollutants or unwanted particles could also enter the nasal airway and deposit in the turbinate region. Deposition of the hazardous particles in the turbinate region might cause possible adverse health effects in the human nasal airway.

Comparison of Nasal Deposition for Fiber and Spherical Aerosol

Aerosol deposition experiments in the nasal airway have been conducted intensively with spherical particles in the inertia regime (Swift 1991; Cheng et al. 1999, 2001a,b; Zwartz and Guilmette 2001; Kelly et al. 2004). It has been shown that most of the experimental data acquired from those studies agree well with each other and the data are all located within a narrow band when the impaction parameter is plotted against the deposition efficiency as shown in Su and Cheng (2005). In this research, deposition experiments were also carried out with spherical particles having comparable aerodynamic diameters to TiO_2 and glass fibers. The aerosol of the spherical particles was generated by the same method as used for generating TiO_2 fiber aerosol (medication nebulizer, as shown in Figure 2). Fluorescent polymer microspheres (Duke Scientific Co., Palo Alto, CA) with sizes ranging from 2.1 to 5.0 μm (d_{ae} = 2.2 to 5.1 μm) were used. Deposition experiments were conducted using a similar experimental method as for the fiber study and the deposition information was acquired by measuring the florescence intensity of the washed-out solution from each nasal airway region. The data obtained were compared with the results from fiber deposition experiments, thereby trying to find the possible differences

TABLE 2
Comparison of the regional deposition fractions and the regional deposition efficiencies for different man-made fiber materials in the human nasal airway

	Anterior		Turbinate		Posterior	
	Dep. fraction (%)	Dep. efficiency	Dep. fraction (%)	Dep. efficiency	Dep. fraction (%)	Dep. efficiency
Carbon Fiber length: 10–40 μm						
15 l/min	35.3	0.35	30.6	0.47	1.0	0.03
30 l/min	77.4	0.77	19.6	0.87	0.5	0.15
43.5 l/min	82.6	0.83	17.2	0.99	0.1	0.51
TiO_2 Fiber length: 2–4 μm						
15 l/min	2.3	0.02	4.9	0.05	0.0	0.00
30 l/min	2.1	0.02	3.5	0.04	1.4	0.01
43.5 l/min	2.7	0.03	6.3	0.07	1.0	0.01
Glass Fiber length: 4–6 μm						
15 l/min	1.0	0.01	2.4	0.02	0.1	0.00
30 l/min	1.3	0.01	1.3	0.01	0.3	0.00
43.5 l/min	2.9	0.03	5.1	0.05	0.2	0.00
Carbon Fiber length: 70–100 μm						
15 l/min	47.7	0.51	33.8	0.66	0.9	0.05
30 l/min	87.7	0.88	11.8	0.96	0.2	0.36
43.5 l/min	82.5	0.82	17.4	0.99	0.1	0.72
TiO_2 Fiber length: 6–8 μm						
15 l/min	1.8	0.02	3.3	0.03	0.0	0.00
30 l/min	7.0	0.07	9.8	0.11	3.8	0.05
43.5 l/min	1.8	0.02	2.0	0.02	0.6	0.01
Glass Fiber length: 8–10 μm						
15 l/min	0.0	0.00	4.3	0.04	0.0	0.00
30 l/min	1.8	0.02	2.5	0.03	0.2	0.00
43.5 l/min	4.8	0.05	5.0	0.05	0.1	0.00

in the aerosol behavior between fiber and spherical particles in the nasal airway. Figure 5 shows the deposition efficiency and some corresponding deposition patterns for fiber aerosol and polymer spherical particles in the nasal airway. As can be seen, for all carbon fibers and spherical particles with a large impaction parameter ($\geq$15,000 $\mu m^2 cm^3/s$), the deposition efficiencies are at least 0.5 and above, and the fiber deposition efficiencies are smaller than the spherical particle deposition efficiencies. In this impaction parameter regime, the anterior region is the site of preferred deposition. In contrast, for those TiO_2 fibers, glass fibers, and spherical particles with a small impaction parameter ($\leq$5,000 $\mu m^2 cm^3/s$), the deposition efficiencies are generally small in the nasal airway (less than 0.2), and relatively higher deposition was found in the turbinate region. However, in this impaction parameter regime, no significant difference was found regarding the deposition efficiency between the fiber aerosol and the spherical particles. The fiber deposition efficiencies were shown to be fairly close to those of spherical particles. The results shown above imply that, in the inertia regime, fibers with low momentum would have similar deposition behavior as do spherical particles having comparable aerodynamic diameters in the human nasal airway during normal breathing, while fibers with high momentum behave differently from spherical particles having an equal aerodynamic diameter.

As stated in Kelly et al. (2004), nasal deposition can be expressed by the following expression:

$$E = 1 - \exp\left[- \left(\alpha d_{ae}^2 Q\right)^{\beta} \right] \quad [1]$$

where α and β are constants needed to be determined. In this study, Equation (1) was adopted and an attempt was made to find the best fit equations for fiber and spherical particle data. A nonlinear fitting procedure in SigmaPlot (SPSS Inc., Chicago, IL) was used as the fitting tool. Recent published spherical particle data from Kelly et al. (2004), Su and Cheng (2005), and the current study were used in the fitting process. It is worth noting that the nasal replicas for these studies were all made from the same MRI scans. Figure 6 shows the best-fit ($\alpha = 6.426 \times 10^{-5}$, $\beta = 1.89$, and $R^2 = 0.90$) curve for the spherical particles, and it was found that this best-fit curve is similar to the curve for

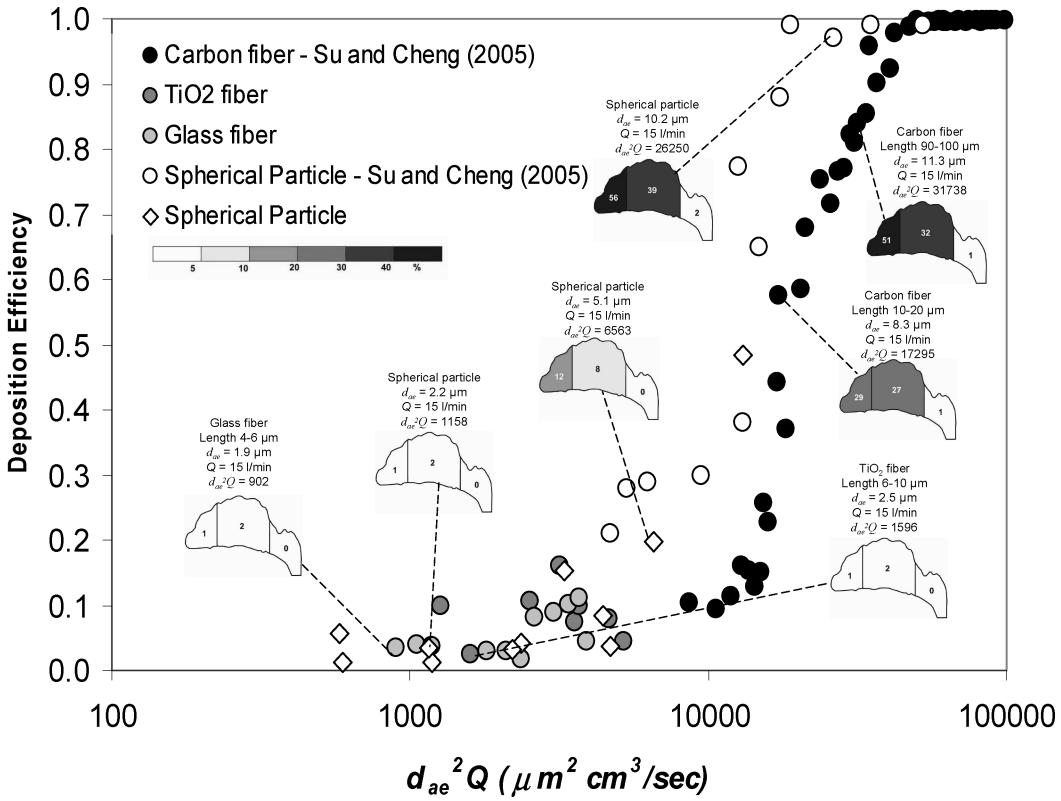

FIG. 5. Comparison of the deposition efficiencies and related deposition patterns between fibers and spherical particles.

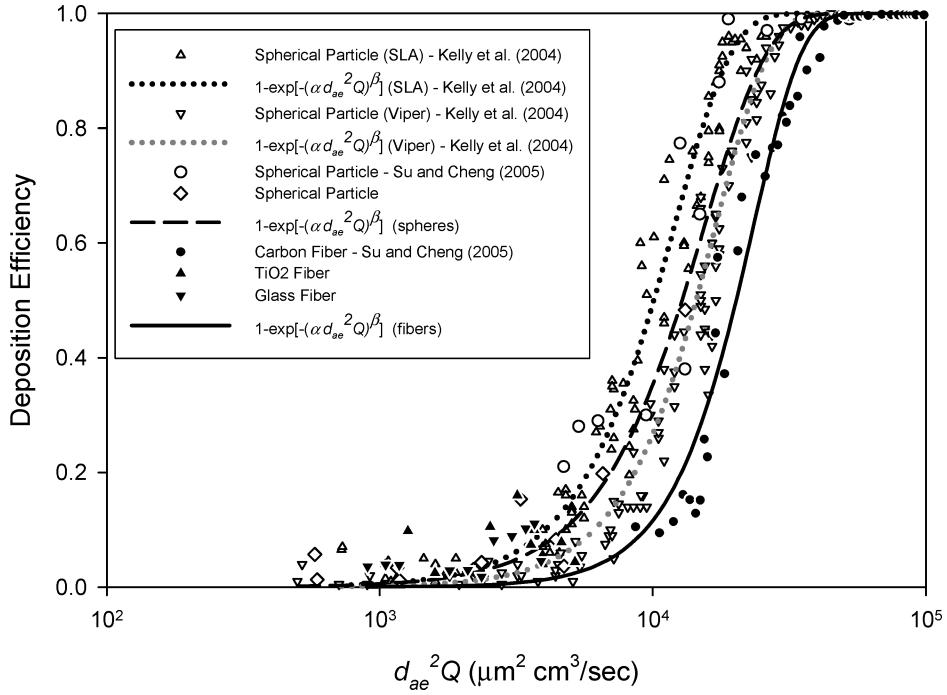

FIG. 6. The best-fit equations of the nasal deposition for fibers and spherical particles.

the Viper nasal replica described in Kelly et al. (2004). In the same way, Equation (1) was used to fit the nasal deposition data for the man-made fibers including carbon, TiO_2, and glass. The best fit curve ($\alpha = 4.262 \times 10^{-5}$, $\beta = 2.46$, and $R^2 = 0.98$) is also plotted in Figure 6 as well as the related fiber experimental data. From this data analysis it is clearly shown that, given the same impaction parameter, fibers deposit less in the human nasal airway and therefore could penetrate more easily into the lower respiratory tract.

CONCLUSION

In this research, deposition efficiencies and deposition patterns in the nasal airway were compared among three man-made fiber materials (carbon, TiO_2, and glass). The result showed that fibers having a large impaction parameter (e.g., carbon fiber) tend to deposit in the anterior region. The deposition mechanism for these large-impaction-parameter fibers is impaction and the deposition efficiency increases as the impaction parameter increases. In contrast, there was no significant deposition mechanism shown for fibers having a small impaction parameter (e.g., TiO_2 and glass fibers). Most of the small-impaction-parameter fibers could easily pass through the entire nasal airway, and relatively more fibers deposited in the turbinate region. Also in this research, fibers and spherical particles with comparable aerodynamic diameters were compared, and best-fit equations were found for both fibers and spherical particles in the nasal airway. It has been shown in this research that small fibers and spherical particles in the inertia regime having same aerodynamic diameters would have similar deposition behavior in the nasal airway, while large fibers were found to have lower deposition than large spherical particles with equal aerodynamic diameters.

REFERENCES

Baan, R. A., and Grosse, Y. (2004). Man-Made Mineral (Vitreous) Fibres: Evaluations of Cancer Hazards by the IARC Monographs Programme, *Mutat. Res.* 553:43–58.

Beeckmans, J. M. (1972). Deposition of Ellipsoidal Particles in the Human Respiratory Tract, in *Assessment of Airborne Particles,* T. T. Mercer, et al. eds., Thomas, Springfield, IL.

Cheng, Y. S., Powell, Q. H., Smith, S. M., and Johnson, N. F. (1995). Silicon Carbide Whiskers: Characterization and Aerodynamic Behavior, *Am. Ind. Hyg. Assoc. J.* 56:970–978.

Cheng, Y. S., Zhou, Y., and Chen, B. T. (1999). Particle Deposition in a Cast of Human Oral Airways. *Aerosol Sci. Technol.* 31:286–300.

Cheng, Y. S., Fu, C. S., Yazzie, D., and Zhou, Y. (2001a). Respiratory Deposition Patterns of Salbutamol pMDI with CFC and HFA-134a Formulations in a Human Airway Replica, *J. Aerosol Med.* 14(2):255–266.

Cheng, Y. S., Holmes, T. D., Gao, J., Guilmette, R. A., Li, S., Surakitbanharn, Y., and Rowlings, C. (2001b). Characterization of Nasal Spray Pumps and Deposition Pattern in a Replica of Human Nasal Airway, *J. Aerosol Med.* 14(2):267–280.

Cole, P. (1982). Upper Respiratory Airflow. In *The Nose*, *Upper Airway Physiology and the Atmospheric Environment*, D. F. Proctor and I. Andersen eds., New York, Elsevier Biomedical Press, pp. 163–189.

Enterline, P. E., Marsh, G. M., Henderson, V., and Callahan, C. (1987). Mortality Update of a Cohort of U.S. Man-Made Mineral Fibre Workers, *Ann. Occup. Hyg.* 31:625–656.

Hesterberg, T. W., and Hart, G. A. (2001). Synthetic Vitreous Fibers: A Review of Toxicology Research and Its Impact on Hazard Classification, *Crit. Rev. Toxicol.* 31:1–53.

Heyder, J., and Rudolph, G. (1977). Deposition of Aerosol Particles in the Human Nose. In *Inhaled Particles IV, Part I*, W. H. Walton, ed., Pergamon Press, New York, NY, pp.107-125.

IARC (2002). IARC Monographs on the Evaluation of Carcinogenic Risks to Humans, Vol. 81, Man-Made Vitreous Fibers. IARC *Press*, Lyon, France.

Kelly, J. T., Asgharian, B., Kimbell, J., and Wong, B. A. (2004). Particle Deposition in Human Nasal Airway Replicas Manufactured by Different Methods. Part I: Inertial Regime Particles, *Aerosol Sci. Technol.* 38:1036–71.

Lippmann, M. (1970). Deposition and Clearance of Inhaled Particles in the Human Nose, *Ann. Otol. Rhinol. Laryngol.* 79(3):519–28.

Lippmann, M. (1977). Regional Deposition of Particles in the Human Respiratory Tract. In *Handbook of Physiology-Reaction to Environmental Agents*, D. H. K. Lee et al. eds., American Physiological Society, Bethesda, MD, pp. 213–232.

Mygind, N. (1985). Upper Airway: Structure, Function and Therapy, in *Aerosol in Medicine. Principles, Diagnosis and Therapy*, F. Moren et al., eds., Elsevier Science Publishers, New York, NY, pp. 1–20.

NCRP (1997). National Council on Radiation Protection and Measurement. *Deposition, Retention and Dosimetry of Inhaled Radioactive Substances*, NCRP Report No. 125, National Council on Radiation Protection and Measurement, Bethesda, MD.

Proctor, D. F. (1982). The Upper Airway, in *The Nose. Upper Airway Physiology and the Atmospheric Environment,* D. F. Proctor et al., eds., Elsevier Science Publishers, New York, pp. 23–43.

Stöber, W., Flachsbart, H., and Hochrainer, D. (1970). The Aerodynamic Diameter of Latex Aggregates and Asbestos Fibres, *Staub-Reinhalt Luft*, 30:1–12.

Stöber, W. (1972). Dynamic Shape Factors of Nonspherical Aerosol Particles, In *Assessment of Airborne Particles,* T. Mercer et al., eds., Charles C. Thomas Publisher, Springfield, IL, 249–89.

Su, W. C., and Cheng, Y. S. (2005). Deposition of Fiber in the Human Nasal Airway, *Aerosol Sci. Technol.* 39:888–901.

Swift, D. L. (1991). Inspiratory Inertial Deposition of Aerosols in Human Nasal Airway Replicate Casts: Implication for the Proposed NCRP Lung Model, *Rad. Prot. Dosimetry*, 38(1/3):29–34.

Swift, D. L., and Proctor D. F. (1977). Access of Air to the Respiratory Tract. In *Respiratory Defense Mechanisms: Part I*, J. D. Brian , D. F. Proctor, and L. M. Reid eds., Dekker, New York, pp. 63–93.

Timbrell, V. (1982). Deposition and Retention of Fibers in the Human Lung, *Ann. Occp. Hyg.* 26:347–369.

Walton, W. H. (1982). The Nature, Hazards, and Assessment of Occupational Exposure to Airbone Asbestos Dusts: A Review, *Ann. Occup. Hyg.* 20:19–23.

Willeke, K., and Baron, P. A. (1993). Measurement of Asbestos and Other Fibers. in *Aerosol Measurement: Principles Techniques and Applications,* K. Willeke and P. A. Baron eds., John Wiley & Sons, Inc., New York, NY, pp. 560–590.

Zamankhan, P., Ahmadi, G., Wang, Z., Hopke, P. K., Cheng, Y. S., and Su, W.C. (2006). Airflow and Deposition of Nano-Particles in a Human Nasal Cavity, *Aerosol Sci. Technol.* 40:463–76.

Zwartz, G. J., and Guilmette, R. A. (2001). Effect of Flow Rate on Particle Deposition in a Replica of a Human Nasal Airway, *Inhal. Toxicol.* 13:109–27.